Identification of a Membrane Fusion Domain and an Oligomerization Domain in the Baculovirus GP64 Envelope Fusion Protein

SCOTT A. MONSMA AND GARY W. BLISSARD*

Boyce Thompson Institute for Plant Research, Cornell University, Tower Road, Ithaca, New York 14853-1801

The baculovirus GP64 envelope fusion protein (GP64 EFP) is the major envelope glycoprotein of the budded virion and has been shown to mediate acid-triggered membrane fusion both in virions and when expressed alone in transfected cells. Using site-directed mutagenesis and functional assays for oligomerization, transport, and membrane fusion, we localized two functional domains of GP64 EFP. To identify a fusion domain in the GP64 EFP of the *Orgyia pseudotsugata* multiple nuclear polyhedrosis virus (Op*M*NPV), we examined two hydrophobic regions in the GP64 EFP ectodomain. Hydrophobic region I (amino acids 223 to 228) is a cluster of 6 hydrophobic amino acids exhibiting the highest local hydrophobicity in the ectodomain. Hydrophobic region II (amino acids 330 to 338) lies within a conserved region of GP64 EFP that contains a heptad repeat of leucine residues and is predicted to form an amphipathic alpha-helix. In region I, nonconservative amino acid substitutions at Leu-226 and Leu-227 (at the center of the hydrophobic cluster) completely abolished fusion activity but did not prevent GP64 EFP oligomerization or surface localization. To confirm the role of region I in membrane fusion activity, we used a synthetic 21-amino-acid peptide to generate polyclonal antibodies against region I and demonstrated that antipeptide antibodies were capable of both neutralizing membrane fusion activity and reducing infectivity of the virus. In hydrophobic region II, mutations were designed to disrupt several structural characteristics: a heptad repeat of leucine, a predicted alpha-helix, or the local hydrophobicity along one face of the helix. Single alanine substitutions for heptad leucines did not prevent oligomerization, transport, or fusion activity. However, multiple alanine substitutions or proline (helix-destabilizing) substitutions disrupted both oligomerization and transport of GP64 EFP. In addition, a deletion that removed region II and the predicted alpha-helix was defective for oligomerization, whereas a larger deletion that retained region II and the predicted helix was oligomerized. These results indicate that region II is required for oligomerization and transport and suggest that the predicted helical structure of this region may be important for this function. Thus, by using mutagenesis, functional assays, and antibody inhibition, two functional domains were localized within the baculovirus GP64 EFP: a fusion domain located at amino acids 223 to 228 and an oligomerization domain located at amino acids 327 to 335 within a predicted amphipathic alpha-helix.

Entry of enveloped viruses into host cells requires fusion of the viral envelope with the host cell membrane. This membrane fusion event is typically accomplished by the action of viral envelope fusion proteins (reviewed in reference 34). Where envelope-membrane fusion occurs at the cell surface, viral fusion proteins typically are active at neutral pH. However, in viruses that enter via receptor-mediated endocytosis, fusion protein activity is most often triggered by the acidic pH within the endosome. Viral fusion proteins often contain hydrophobic domains or fusion peptides that are important for membrane fusion activity. These hydrophobic domains presumably interact with the hydrophobic lipid interior of the host cell membranes and are typically conserved within but not between virus families (34). Fusion peptides may be internal, or they may occur at the N terminus of the fusion protein (34). In several cases, N-terminal fusion peptides are also flanked by potential amphipathic alpha-helical regions containing a-d repeat sequences, which have the potential to form coiled-coils of multiple helices (7). A role for amphipathic alpha-helices in membrane fusion activity has been demonstrated in the mea-

sles virus fusion (F) protein and the human immunodeficiency virus type 1 transmembrane protein gp41 (5, 11).

The baculovirus GP64 envelope fusion protein (GP64 EFP) is the major envelope protein of the budded virion. The native GP64 EFP is a phosphoglycoprotein found at the surfaces of infected cells and in virions (23, 31; reviewed in reference 30). GP64 EFP is a type I integral membrane protein, bearing a signal peptide at the N terminus and a 23-amino-acid hydrophobic transmembrane domain near the C terminus (2). In addition to carbohydrate modification, GP64 EFP is fatty acid acylated near the transmembrane domain (24). The GP64 EFP open reading frame (ORF) of the *Autographa californica* multiple nuclear polyhedrosis virus (Ac*M*NPV) encodes a protein of 511 amino acids (35), whereas those of the *Orgyia pseudotsugata* and *Choristoneura fumiferana* multiple nuclear polyhedrosis viruses (Op*M*NPV and Cf*M*NPV) both encode proteins of 509 amino acids (2, 13). The amino acid sequence of GP64 EFP is highly conserved between these three baculoviruses, exhibiting identities of 88% between the GP64 EFPs of Op*M*NPV and Cf*M*NPV, 78% between the GP64 EFPs of Ac*M*NPV and Op*M*NPV, and 80% between the GP64 EFPs of Cf*M*NPV and Ac*M*NPV. Op*M*NPV GP64 EFP contains 16 cysteine residues (14 in the ectodomain [2]), and intersubunit disulfide bonds participate in the formation of the native oligomeric structure (31). Peplomers visible at the surfaces of budded virions

* Corresponding author. Mailing address: Boyce Thompson Institute, Cornell University, Tower Rd., Ithaca, NY 14853-1801. Phone: (607) 254-1366. Fax: (607) 254-1242. Electronic mail address: gwb1@cornell.edu.

in transmission electron micrographs are believed to consist of homo-oligomers of GP64 EFP (27) and are stained by antibodies directed against GP64 EFP (33).

GP64 EFP is required for productive infection, as monoclonal antibodies (MAbs) directed against GP64 EFP can neutralize budded virion infectivity (14, 23). Earlier it was demonstrated that a neutralizing MAb directed against GP64 EFP, AcV1, does not interfere with binding or uptake of virions into host cells but blocks infection at a later stage (32). Infection by baculovirus budded virions can also be prevented by treatment with agents that prevent acidification of the endosome, such as chloroquine or ammonium chloride (16, 32). This indicates that baculovirus budded virions enter host cells by the endocytotic pathway. More recently, it was shown that acid pH induces fusion of baculovirus-infected cells which display GP64 EFP on their surfaces (4, 18). In addition, GP64 EFP transiently expressed from a plasmid in uninfected cells mediates this acid-induced membrane fusion (4), indicating that GP64 EFP alone is sufficient for the membrane fusion event of the viral envelope with the endosomal membrane.

In the studies reported here, we used transient expression in combination with mutagenesis, functional assays, and antibody inhibition to identify two functional domains of the baculovirus GP64 EFP.

MATERIALS AND METHODS

Epitope library construction. Two MAbs (AcV5 and B12D5) (14, 15) are routinely used to detect wild-type (wt) and modified forms of Op*M*NPV and Ac*M*NPV GP64 EFPs. To facilitate the analysis of modified GP64 EFP, the epitopes recognized by these MAbs were mapped. To generate an epitope library, DNA from the coding region of the Ac*M*NPV *gp64 efp* gene was randomly digested in the presence of 10 mM Mn^{2+} (1), to an average size of approximately 30 to 90 bp. The digestion products were repaired with *Taq* polymerase (Promega), cloned as fusions into the T7 gene 10 reading frame in the pTOPE bacterial expression vector (Novagen), and transformed into the NovaBlue(DE3) bacterial strain (Novagen). Colony lifts were immunologically screened with tissue culture supernatants from hybridoma cell lines AcV5 and B12D5. Positive clones were isolated and rescreened, and the inserts were sequenced by using a T7 terminator primer (Novagen).

Linkers and site-specific mutagenesis. For studies of mutations in the Ac*M*NPV GP64 EFP, the Ac*M*NPV GP64 EFP ORF was cloned into plasmid p166B+1, under the control of the same promoter used for previous studies of the Op*M*NPV GP64 EFP (4). Plasmid p166B+1 contains promoter sequences, a *Bam*HI cloning site, and downstream untranslated sequences containing polyadenylation signals. The promoter consists of the Op*M*NPV *gp64 efp* promoter region beginning 166 bp upstream of the GP64 EFP translation initiation codon (−166 to +1, with +1 defined as the "A" of the GP64 EFP translation initiation codon). A *Bam*HI linker (5′-CCGGATCCGG-3′) was inserted after position +1 of the GP64 EFP translation initiation codon. The *Bam*HI linker was immediately followed by 180 bp of *gp64 efp* 3′ untranslated sequences containing the *gp64 efp* cleavage-polyadenylation signals (from the *Acc*I restriction site at +1620 to the *Bam*HI restriction site at +1811 of plasmid p64CAT-166 [3]). The Ac*M*NPV GP64 EFP ORF was isolated as a 1,726-bp *Spe*I-*Bgl*I restriction fragment from a plasmid containing the *Eco*RI H fragment of the Ac*M*NPV (strain E2) genome (25). The GP64 EFP ORF begins 49 bases downstream of the *Spe*I cleavage site and terminates 145 bases upstream of the *Bgl*II cleavage site. The *Bgl*II end of the 1,726-bp fragment was ligated into the unique *Bam*HI site of p166B+1, and the incompatible overhanging *Spe*I and *Bam*HI ends were filled in by using the large fragment of DNA polymerase I (Klenow fragment) and deoxynucleotides. The resulting blunt ends were ligated, and the plasmid was named p166B+1 Ac Spe/Bgl.

For linker insertion mutagenesis, linkers encoding 6 amino acids were designed to avoid stop codons in all possible reading frames. A blunt-ended double-stranded DNA linker containing *Bgl*II, *Kpn*I, and *Hin*dIII restriction sites (BKH linker, 5′-AGATCTGGTACCAAGCTT-3′ and 5′-AAGCTTGGTACCAGATCT-3′) was synthesized and inserted into the *Nru*I, *Kas*I, or *Nae*I restriction site of the Ac*M*NPV GP64 EFP ORF in plasmid p166B+1 Ac Spe/Bgl. Similarly, a blunt-ended double-stranded linker containing *Sal*I, *Sph*I, and *Xho*I restriction sites (SSX linker, 5′-GTCGACGCATGCCTCGAG-3′ and 5′-CTCGAGGCAT GCGTCGAC-3′) was inserted into the *Nae*I, *Tth*111I, *Nsi*I, or *Hin*cII restriction site of the Op*M*NPV GP64 EFP ORF in plasmid p64-166 (4). To maintain the GP64 EFP ORF, the Op*M*NPV *Tth*111I restriction site and the Ac*M*NPV *Kas*I restriction site were filled in with Klenow fragment and deoxynucleotides prior to linker insertion. A modified double-stranded SSX linker with *Pst*I-compatible ends (P-SSX-P linker, 5′-GGTCGACGCATGCCTCGAGATGCA-3′ and 5′-

TCTCGAGGCATGCGTCGACCTGCA-3′) was also inserted into the *Pst*I site of the Op*M*NPV GP64 EFP ORF in plasmid p64-166 to generate plasmid p64-166 Pst(P-SSX-P).

For site-directed mutagenesis in the Op*M*NPV *gp64 efp* gene, we used the long primer unique-site elimination PCR protocol (22). To generate amino acid substitution mutations, the primer 5′-ATACGACTCACTATAGGGCGt ATTC-3′ was used to eliminate the unique *Eco*RI restriction site in the multiple cloning site of plasmid p64-166, in combination with the following mutagenic primers (mismatched bases are shown in lowercase; s = g and c):

Region I

L226D/L227D,	5′-AGCTTGCgatgaCATTAAAGACG-3′
L226A/L227A,	5′-AGCTTGCgcGgcCATTAAAGACG-3′
C225S,	5′-AGCTTcCTTGCTCATTAAAGACG-3′
L226M/L227M,	5′-AGCTTGCaTGaTgATTAAAGACG-3′
L226M,	5′-AGCTTGCaTGCTCATTAAAGACG-3′
L226A,	5′-AGCTTGCgcGCTCATTAAAGACG-3′
L227M,	5′-AGCTTGCTTGaTgATTAAAGACG-3′
L227A,	5′-AGCTTGCTTGgcCATTAAAGACG-3′

Region II

L327A or L327P,	5′-CAACAAAscAAACAACATGATGC-3′
L334A or L334P,	5′-GCACGATscGATTGTGTCGGTGG-3′
L327A/L334A,	5′-CAACAAAgcAAACAACATGATGCACGATgcGATTGTGTCG-3′
L327P/L334P,	5′-CAACAAAccAAACAACATGATGCACGATccGATTGTGTCG-3′
M330A/M331A/L334A/I335A,	5′-AAACAACgcGgcGCACGATgcGgcTGTGTCGGTG-3′

Mutations were generated in the wt Op*M*NPV GP64 EFP expression vector plasmid p64-166 and sequenced to confirm the presence of the desired mutations. To eliminate the possibility of inadvertent mutations in other regions of the *gp64 efp* gene (from PCR errors), small restriction fragments bearing the desired mutations were subcloned into the wt p64-166 plasmid. Each region I mutation was subcloned as a 176-bp *Tth*111I-*Nsi*I restriction fragment (see sites shown in Fig. 2A), and each region II mutation was subcloned as a 235-bp *Nsi*I-*Hin*cII restriction fragment (see Fig. 2A). Mutations within the inserts and the restriction site junctions were again verified by sequencing in both directions, using primers adjacent to the cloning sites. A 250-amino-acid deletion in the Ac*M*NPV GP64 EFP ORF was constructed by digestion of p166B+1 Ac Spe/Bgl with *Bbs*I and *Eag*I (see Fig. 9B), removal of the 750-bp fragment (encoding amino acids 29 to 278), and religation of the blunt ends, resulting in plasmid p166B+1 Ac ΔBE. A 77-amino-acid deletion in the Op*M*NPV GP64 EFP ORF was constructed from plasmid p64-166 Nsi(SSX), which was derived from plasmid p64-166 by insertion of the SSX linker at the *Nsi*I site (see Fig. 2A). Plasmid p64-166 Nsi(SSX) was digested with *Hin*cII (which cleaves between the first two codons of the SSX linker and at the *Hin*cII restriction site between amino acids 341 and 342), and the compatible ends were religated. The result was a GP64 EFP protein with a deletion of amino acids 264 to 340 of the wt Op*M*NPV GP64 EFP sequence. This plasmid was named p64-166 ΔLZ.

Insect cells and transfections. Insect Sf9 cells (a clonal derivative of the IPLB-Sf21 cell line) were cultured as previously described (21, 26). Transfections were performed in 24-well plates by using 3.75 μg of CsCl-purified supercoiled plasmid DNA in each well containing 3×10^5 Sf9 cells (3). After transfection, cells were incubated at 27°C for 48 h to allow expression and transport of GP64 EFP to the cell surface. Replicate wells were processed in parallel for the following assays: (i) oligomerization analysis by Western immunoblots of nonreducing sodium dodecyl sulfate (SDS)-polyacrylamide gels, (ii) surface localization of GP64 EFP by cell surface enzyme-linked immunosorbent assay (CELISA), and (iii) membrane fusion activity by syncytium formation assay.

Oligomerization, surface localization, and membrane fusion assays. To examine the oligomerization state of GP64 EFP, proteins from transfected cells were denatured and electrophoresed under nonreducing conditions. Transfected cells were rinsed twice in phosphate-buffered saline (PBS), pH 7.4 (Sigma), and lysed in buffer containing 25 mM Tris-HCl, (pH 6.8), 1% SDS, 15% glycerol, and 37.5 mM iodoacetamide (28, 31). Samples were electrophoresed on 6% SDS-polyacrylamide gels (17) and transferred to an Immobilon-P membrane (Millipore) by using a semidry electrotransfer apparatus. GP64 EFP was detected by incubation with MAb AcV5 as previously described (4).

To obtain a quantitative comparison of wt and mutant GP64 EFPs at the cell surface, relative levels of surface-localized GP64 EFP were determined by a CELISA. Transfected cells were rinsed twice in PBS and fixed at room temperature (RT) for 30 min in fresh 4% (wt/vol) paraformaldehyde in PBS. Fixed cells were rinsed twice in Tris-buffered saline (TBS; 20 mM Tris-HCl, 0.5 M NaCl, pH 7.5) and blocked for 1 h with 1% (wt/vol) gelatin in TBS. Surface GP64 EFP was detected with MAb AcV5 (ascites fluid diluted in 0.5% [wt/vol] gelatin in TBS), alkaline phosphatase conjugated to goat anti-mouse immunoglobulin G (Promega; diluted in 0.5% gelatin–TBS), and the chromogenic substrate *p*-nitrophenyl phosphate (Boehringer) at 10 mg/ml in alkaline buffer (100 mM Tris-HCl, 100 mM NaCl, 5 mM $MgCl_2$ [pH 9.5]).

The syncytium formation assay for membrane fusion activity was performed essentially as described previously (4). Transfected cells were rinsed once with PBS adjusted to pH 5.0 (with citric acid) and then incubated in PBS at pH 5.0 for 5 min at RT. The acidic buffer was withdrawn and replaced with fresh tissue culture medium (TNM-FH at pH 6.1 [26]), and the cells were incubated at 27°C for 2 h. Cultures were scored as positive for syncytium formation if syncytia containing more than five nuclei were present. For antibody inhibition of fusion

activity, Sf9 cells were transfected with plasmid p64-166 (encoding wt Op*M*NPV GP64 EFP). At 48 h posttransfection, the cells were incubated with the following in PBS-citrate buffer (pH 6.5): (i) affinity-purified antipeptide antibodies (0.75 mg/ml), (ii) affinity-purified antipeptide antibodies (0.75 mg/ml) plus region I peptide (1 mg/ml), or (iii) region I peptide (1 mg/ml). After incubation for 1 h at RT, the cells were tested in the syncytium formation assay as described above.

Synthetic peptide and antipeptide antibodies. A region I peptide corresponding to Op*M*NPV GP64 EFP amino acids 222 to 241 (see Fig. 5A) was synthesized and purified by high-performance liquid chromatography. The peptide was conjugated via the tyrosine hydroxyl group to keyhole limpet hemocyanin (Pierce) by using bis-diazotized benzamidine (12). A polyclonal antiserum directed against the keyhole limpet hemocyanin-conjugated peptide was generated in a rabbit. For affinity purification of peptide-specific antibodies, the peptide was conjugated at pH 11 to epoxy-activated agarose beads (Pierce) via the tyrosine hydroxyl group. Antibodies were bound by incubating the beads with crude serum diluted 1:10 in PBS (pH 7.4). Antipeptide antibodies were eluted from the beads with 100 mM glycine (pH 3.0) followed by 100 mM glycine (pH 2.5).

Virus and viral infectivity assay. Because GP64 EFP is expressed as an early gene product during infection, we used GP64 EFP expression in Op*M*NPV-infected *Lymantria dispar* cells (Ld652Y) as a measure of viral entry into host cells for neutralization experiments. In this assay, early expression of GP64 EFP in Op*M*NPV-infected *L. dispar* cells is proportional to the number of virions entering host cells or input gene dosage. To demonstrate this relationship and to generate a standard curve of GP64 EFP expression as a function of multiplicity of infection (MOI), an Op*M*NPV budded virus stock (1.75×10^8 infectious units per ml) was diluted to yield a range of MOIs from 0.01 to 10. *L. dispar* cells were plated in 24-well dishes at 3.5×10^5 cells per well and infected by incubating with diluted virus for 1 h at RT with gentle rocking. After the 1-h infection period, cells were rinsed twice with TNM-FH medium and fresh medium was added. Infected cells were incubated for 20 h at 27°C and then rinsed twice with PBS and fixed with 100% methanol, a fixation that simultaneously permeabilizes the cells. GP64 EFP was detected by CELISA as described above. To control for GP64 EFP from the viral inoculum, infected cell controls were fixed and analyzed by CELISA immediately after the 1-h infection period. No GP64 EFP from the viral inoculum was detected at MOIs of ≤20.

For antibody neutralization of infectivity, 32 μl of Op*M*NPV virus stock (1.75×10^8 infectious units per ml) was mixed either with 200 μl of buffer (PBS-citrate [pH 6.5]) or with 200 μl of the following in PBS-citrate buffer: (i) affinity-purified antipeptide antibodies (0.75 mg/ml), (ii) affinity-purified antipeptide antibodies (0.75 mg/ml) plus region I peptide (1 mg/ml), or (iii) region I peptide (1 mg/ml). Each virus treatment (antibody, antibody plus peptide, or peptide) was incubated for 1 h at RT and then diluted to 800 μl with TNM-FH medium and used to infect *L. dispar* cells. For infections with treated virus, 250 μl of the diluted virus was added to *L. dispar* cells (3.6×10^5 cells per well) and incubated for 1 h at RT with gentle rocking. Cells were fixed at 20 h postinfection and analyzed by CELISA as described above.

RESULTS

Epitope mapping. The baculovirus GP64 EFP is required for budded virus entry into host cells (14, 23, 33) and was previously shown to encode a membrane fusion activity (4). In this study, mutagenesis and functional assays were used to localize functional domains required for the acid-induced membrane fusion activity of GP64 EFP and for the oligomerization of GP64 EFP. Because MAbs were used to detect GP64 EFP in this study, we first mapped the epitopes of two MAbs (AcV5 and B12D5) which were previously raised against the Ac*M*-NPV GP64 EFP (14, 15). Previous studies (14, 15) found that both AcV5 and B12D5 reacted with denatured GP64 EFP on Western blots, indicating that their epitopes are linear. Therefore, we mapped both epitopes by screening an epitope library expressed in *Escherichia coli*. Four clones were isolated from the epitope library by screening with B12D5, and six clones were isolated by screening with AcV5. The deduced amino acid sequences from the inserts of immunopositive clones are shown aligned below the corresponding amino acid sequences of Ac*M*NPV GP64 EFP (Fig. 1A and B). The B12D5 epitope was mapped to 11 amino acids located at amino acids 277 to 287 of the Ac*M*NPV GP64 EFP sequence (Fig. 1A and C). Within the 11-amino-acid B12D5 epitope region, 7 amino acids are identical between the Ac*M*NPV, Cf*M*NPV, and Op*M*-NPV GP64 EFPs. The AcV5 epitope was mapped to 9 amino acids (amino acids 431 to 439) near the C terminus of Ac*M*-NPV GP64 EFP (Fig. 1B and C). Within the 9-amino-acid

AcV5 epitope region, 8 amino acids are identical between the Ac*M*NPV, Cf*M*NPV, and Op*M*NPV GP64 EFPs.

Surface localization and membrane fusion. Because mutations in GP64 EFP may affect cellular transport of the protein and membrane fusion of transfected cells is dependent on surface localization of GP64 EFP, we used a CELISA protocol to measure relative levels of GP64 EFP at the surfaces of fixed cells. In initial control experiments, we determined the sensitivity of the CELISA for GP64 EFP surface detection and examined the effect of decreasing levels of surface GP64 EFP on the ability to detect membrane fusion. Cells were transfected with decreasing quantities of plasmid encoding wt Op*M*-NPV GP64 EFP (plasmid p64-166), from 40 to 0.1 μg per 3×10^5 cells, and examined with both CELISA and membrane fusion assays. The maximal level of GP64 EFP surface expression (as detected in the CELISA) was obtained by using 3.75 μg of plasmid DNA per 3×10^5 cells. Membrane fusion activity was reproducibly detected when surface GP64 EFP levels were reduced to 20% of the maximal level. Further reduction in surface GP64 EFP resulted in no detectable fusion activity (data not shown).

Since correct folding, oligomerization, and disulfide bonding are likely required for surface localization (10) and fusion activity of GP64 EFP, we assessed the effect of each mutation on oligomerization and disulfide bonding by electrophoresis on nonreducing SDS-polyacrylamide gels, followed by Western blot analysis with MAb AcV5. On nonreducing gels, wt GP64 EFP migrated predominantly as two bands with apparent molecular sizes of approximately 225 and 180 kDa (see Fig. 4A, lane 1). Recent mass spectrometry and gel filtration studies of a purified soluble GP64 EFP indicate that these two bands represent two forms of trimeric GP64 EFP (20a) rather than tetramers and trimers as was previously hypothesized (31). For the purposes of this study, we will therefore refer to the apparent 225-kDa form as trimer I and the apparent 180-kDa form as trimer II.

Insertional mutagenesis. Our initial approach to mapping functional domains of GP64 EFP was insertional mutagenesis. Small oligonucleotide linkers were inserted, in frame, into seven unique restriction sites throughout the coding regions of the Ac*M*NPV and Op*M*NPV *gp64 efp* genes (Fig. 2A), resulting in insertions of 6 to 12 amino acids in the GP64 EFP protein (Fig. 2B, Amino acids). The resulting mutant proteins were expressed in transfected tissue culture cells under the control of the Op*M*NPV *gp64 efp* early promoter, as described previously (4). The results of the linker insertion mutations on GP64 EFP oligomerization, surface localization, and fusion activity are summarized in Fig. 2B. Six of the seven linker insertion mutations resulted in defective oligomerization of GP64 EFP (Fig. 2B, Oligomers) and greatly reduced surface localization of GP64 EFP (≤20% of wt levels; Fig. 2B, Surface) and completely lacked acid-induced membrane fusion activity in the syncytium formation assay (Fig. 2B, Fusion). The lack of fusion activity was not surprising since surface localization was greatly reduced. Only the linker insertion at the *Kas*I restriction site of Ac*M*NPV GP64 EFP appeared to oligomerize properly and retained membrane fusion activity. To determine if smaller amino acid insertions might be tolerated, the unique restriction sites within the linkers were used to delete the central portion of the linker from the four Op*M*NPV GP64 EFP linker insertion mutants. The resulting GP64 EFP proteins contained smaller residual insertions of 2, 3, or 4 amino acids (Fig. 2B, Linker Reductions). Three of the four linker reduction mutations exhibited the same defect in surface localization as the parent linker insertions. Only the reduced linker at the *Nae*I restriction site of Op*M*NPV GP64 EFP

A. MAb B12D5

```
                                              277         287
                                               |           |
AcMNPV GP64 EFP:   ...NCKFNRCIKRKVEHRVKKRPPTWRHNVRAKYTEGDTATKG...
     B23              CKFNRCIKRKVEHRVKKRPPTWRHNVRAKYTEGDTATK
     B11                       KVEHRVKKRPPTWRHNVRAK
     B2                            KKRPPTWRHNVRAKYTEGDTA
     B7                            VKKRPPTWRHNV

Maximal B12D5 epitope region:           KKRPPTWRHNV
```

Baculovirus	
AcMNPV GP64 EFP:	KKRPPTWRHNV
CfMNPV GP64 EFP:	-Q--V----DV
OpMNPV GP64 EFP:	-Q--H----DR

B. MAb AcV5

```
                                              431       439
                                               |         |
AcMNPV GP64 EFP:...KELAIHDVEFWIPTIGNTTYHDSWKDASGWSFIAQQKSNLITTMENTKFGGVGTSLSDIT...
     A1          ...KELAIHDVEFWIPTIGNTTYHDSWKDASGWSFIAQQKSNLITTMENTKFGGVGTSLSDIT...
     A13                          SWKDASGWSFIAQQKSNLITTMENTKFGGVGTSLS
     A8-3                      NTTYHDSWKDASGWSFIAQQKSNLITT
     A6                     TIGNTTYHDSWKDASGWSF
     A9          ...KELAIHDVEFWIPTIGNTTYHDSWKDASGWSF
     A28            ELAIHDVEFWIPTIGNTTYHDSWKDASGWS

Maximal AcV5 epitope region:         SWKDASGWS
```

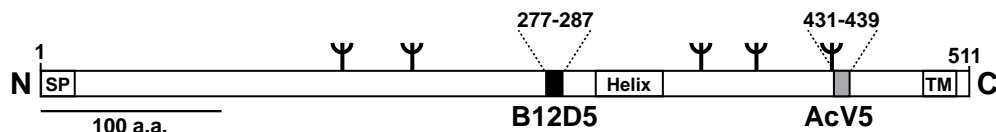| *Baculovirus*	
AcMNPV GP64 EFP:	SWKDASGWS
CfMNPV GP64 EFP:	N--------
OpMNPV GP64 EFP:	S--------

C. AcMNPV GP64 EFP

FIG. 1. Epitope mapping for MAbs B12D5 and AcV5. To map epitopes, an epitope library was constructed from the Ac*M*NPV GP64 EFP ORF and screened with MAbs B12D5 and AcV5. Insert DNAs from immunopositive colonies were sequenced, conceptually translated, and aligned, and a consensus corresponding to a maximal epitope region was derived. (A) Alignment of predicted amino acid sequences encoded by inserts from colonies identified with MAb B12D5 (B23, B11, B2, and B7) resulted in a maximal epitope region of 11 amino acids (underlined). In the lower panel, the B12D5 epitope region from the Ac*M*NPV GP64 EFP is compared with the same region from the Op*M*NPV and Cf*M*NPV GP64 EFPs. B12D5 reacts only weakly with Op*M*NPV GP64 EFP on Western blots (data not shown). Identical amino acids are indicated by dashes. (B) Alignment of six amino acid sequences encoded by inserts from colonies identified with MAb AcV5 (A1, A13, A8-3, A6, A9, and A28) resulted in a maximal epitope region of 9 amino acids (underlined). In the lower part of the panel, the AcV5 epitope region from the Ac*M*NPV GP64 EFP is compared with the same region from the Op*M*NPV and Cf*M*NPV GP64 EFPs. (C) Schematic map of the Ac*M*NPV GP64 EFP amino acid sequence (long box), showing the locations of the B12D5 (black box) and AcV5 (gray box) epitopes in relation to major features of the protein. SP, signal peptide; Helix, predicted alpha-helical region; TM, transmembrane domain; Ψ, predicted N-linked glycosylation sites. Bar, 100 amino acids.

(which resulted in a residual insertion of 2 amino acids) regained surface localization and acid-induced fusion activity. These results suggested that both Ac*M*NPV and Op*M*NPV GP64 EFP were sensitive to small amino acid insertions (2 to 12 amino acids) at a number of sites. These modifications, which altered the internal spacing of GP64 EFP, generally resulted in defective oligomerization and interfered with transport to the cell surface.

Site-directed mutagenesis. Because sensitivity to insertional mutagenesis precluded a comprehensive investigation by that method, we used site-directed mutagenesis to create amino acid substitutions at selected sites within the GP64 EFP sequence. Fusion domains that have been characterized in other viral envelope fusion proteins often involve highly hydrophobic

regions (34). We therefore examined the predicted hydrophobicity profile (20) of Op*M*NPV GP64 EFP (Fig. 3A) and selected, for functional analysis, the two regions of highest local hydrophobicity in the ectodomain. The first hydrophobic region is composed of 6 hydrophobic residues at amino acids 223 to 228 (Fig. 3A, region I, and 3B, light gray box) and is highly conserved between the Ac*M*NPV, Op*M*NPV, and Cf*M*NPV GP64 EFPs. The second hydrophobic region is located at amino acids 330 to 338 (Fig. 3A, II) and lies within a conserved portion of the protein which is predicted to form an amphipathic alpha-helix. Within these two selected hydrophobic regions of the Op*M*NPV GP64 EFP, amino acid substitutions were created by site-directed mutagenesis.

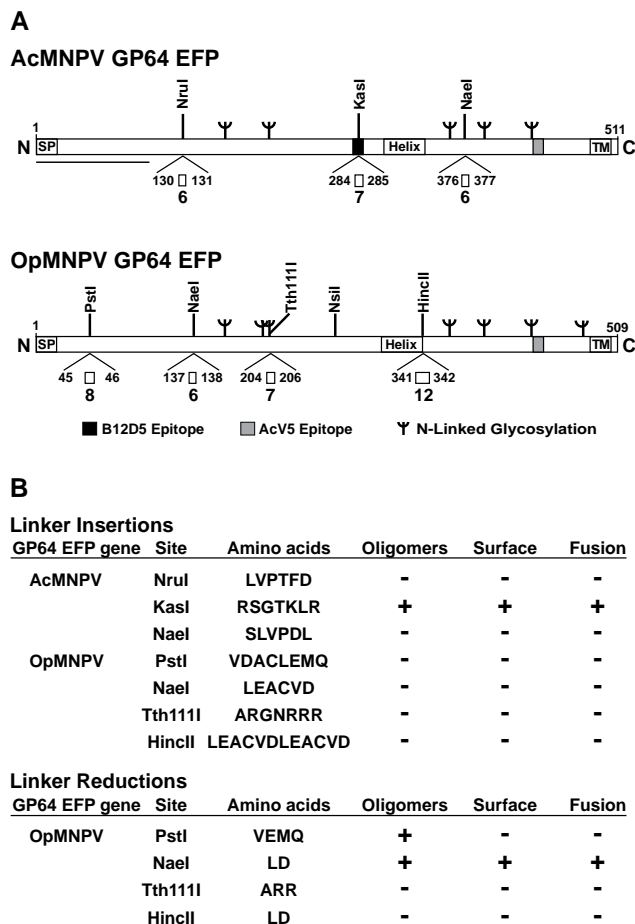**Mutations in hydrophobic region I.** Within hydrophobic re-

A

AcMNPV GP64 EFP

OpMNPV GP64 EFP

■ B12D5 Epitope   ▦ AcV5 Epitope   Ψ N-Linked Glycosylation

B

Linker Insertions

GP64 EFP gene	Site	Amino acids	Oligomers	Surface	Fusion
AcMNPV	NruI	LVPTFD	−	−	−
	KasI	RSGTKLR	+	+	+
	NaeI	SLVPDL	−	−	−
OpMNPV	PstI	VDACLEMQ	−	−	−
	NaeI	LEACVD	−	−	−
	Tth111I	ARGNRRR	−	−	−
	HincII	LEACVDLEACVD	−	−	−

Linker Reductions

GP64 EFP gene	Site	Amino acids	Oligomers	Surface	Fusion
OpMNPV	PstI	VEMQ	+	−	−
	NaeI	LD	+	+	+
	Tth111I	ARR	−	−	−
	HincII	LD	−	−	−

FIG. 2. Linker insertion and linker reduction mutagenesis of Ac*M*NPV and Op*M*NPV GP64 EFPs. (A) Schematic maps of Ac*M*NPV and Op*M*NPV amino acid sequences (long boxes), showing predicted structural features, MAb epitopes (B12D5 and AcV5), and the locations of restriction sites used for linker insertion mutagenesis. Each linker insertion is represented by a small open box below a restriction site in the GP64 EFP ORF. The number below each linker indicates the number of amino acids inserted between the indicated GP64 EFP amino acids (numbers flanking each linker). Bar, 100 amino acids. Abbreviations are explained in the legend to Fig. 1C. (B) Linker insertion sites are listed for each *gp64 efp* gene along with the amino acids encoded by the linker insertion and the effects of the linker insertion on oligomerization, surface localization, and fusion activity. Oligomers: +, distinct trimer I and trimer II bands were detected on Western blots of nonreduced SDS-polyacrylamide gels. Surface: +, CELISA signals of >20% of wt levels; −, CELISA signals of ≤20% of wt levels. Fusion: +, syncytia containing five nuclei or more were detected in the syncytium formation assay.

gion I, the peak of hydrophobicity is contributed by three amino acids, Cys-225-Leu-226-Leu-227 (Fig. 3B, dark gray box). Three strategies were used to examine the role of the hydrophobic leucine residues at positions 226 and 227 (Fig. 3B): (i) reducing the hydrophobicity by substituting alanine for either or both leucines, (ii) drastically altering the hydrophobic character of the region by substituting polar, charged residues (aspartic acid) for both leucine residues, and (iii) retaining the hydrophobicity of the region by substituting a hydrophobic residue of similar bulk (methionine) for either or both leucines.

Leu-226 and Leu-227 contribute substantially to the average hydrophobicity of region I. To reduce the overall hydrophobicity of region I with minimal effects on secondary structure, the neutral amino acid alanine was substituted for either one

or both Leu-226 and Leu-227 (Fig. 3B; L226A, L227A, and L226A/L227A). GP64 EFP containing these substitutions oligomerized into the two trimer forms at levels similar to those of wt GP64 EFP (Fig. 4A, compare lane 1 with lanes 2 to 4). Therefore, oligomerization of GP64 EFP containing these substitutions appeared normal. In the CELISA, both single and double alanine substitutions resulted in near wt levels of GP64 EFP at the cell surface (Fig. 4B, compare column 1 with 2 to 4). In the fusion assay, GP64 EFP containing either of the single alanine substitutions retained membrane fusion activity (Fig. 4C, L226A and L227A). However, GP64 EFP containing the double alanine substitutions at positions 226 and 227 completely lacked detectable membrane fusion activity (Fig. 4C, L226A/L227A). Because GP64 EFP containing the double alanine substitutions was oligomerized and transported to the cell surface yet lacked fusion activity, the acid-induced fusion activity of GP64 EFP appears to depend on the level of hydrophobicity at amino acid positions 226 and 227. We therefore examined further the contribution to hydrophobicity by these two residues.

To radically alter the hydrophobic nature of region I while maintaining the approximate bulk of the leucine side chains, a similar-sized but polar and charged residue (aspartic acid) was substituted for both Leu-226 and Leu-227 (Fig. 3B; L226D/L227D). The double aspartate substitutions at positions 226 and 227 resulted in some apparently minor interference with oligomerization, as indicated by increased levels of monomeric and dimeric GP64 EFP and slightly altered migration of the trimer I and trimer II bands (Fig. 4A, lane 5). However, the double aspartate substitutions did not prevent surface localization, as the mutant GP64 EFP was detected at the surface at approximately 80% of the wt level (Fig. 4B, column 5). In the fusion assay, GP64 EFP containing the double aspartate substitutions completely lacked acid-induced membrane fusion activity (Fig. 4C, L226D/L227D). Thus, GP64 EFP containing either double alanine or double aspartate substitutions at positions 226 and 227 lacked fusion activity, yet exhibited near normal levels of oligomerization and surface localization. Again, these data indicate that the hydrophobicity of Leu-226 and Leu-227 plays an important role in the acid-induced membrane fusion activity of GP64 EFP.

Because substitutions that reduced the hydrophobicity at positions 226 and 227 eliminated fusion activity, we hypothesized that conservative hydrophobic amino acid substitutions at these positions would not abolish fusion activity. To test this hypothesis, the hydrophobic amino acid methionine was substituted for either one or both Leu-226 and Leu-227 (Fig. 3B; L226M, L227M, and L226M/L227M). These substitutions appeared to have little or no effect on oligomerization of GP64 EFP (Fig. 4A, lanes 6 to 8) and did not significantly affect levels of GP64 EFP at the cell surface (Fig. 4B, columns 6 to 8). GP64 EFP containing either of the single methionine substitutions or the double methionine substitutions at positions 226 and 227 retained membrane fusion activity (Fig. 4C, L226M, L227M, and L226M/L227M). Thus, GP64 EFP proteins that contained conservative substitutions (maintaining the hydrophobicity of region I) also retained the acid-induced membrane fusion activity. In combination with the results from the two sets of nonconservative substitutions at these same positions, these data demonstrate that the hydrophobicity of residues 226 and 227 within region I is required for membrane fusion activity.

Cys-225 is both hydrophobic and may form a disulfide bond, and either factor may be important for GP64 EFP fusion activity. To eliminate the potential disulfide bond while maintaining the approximate bulk of the cysteine residue in position
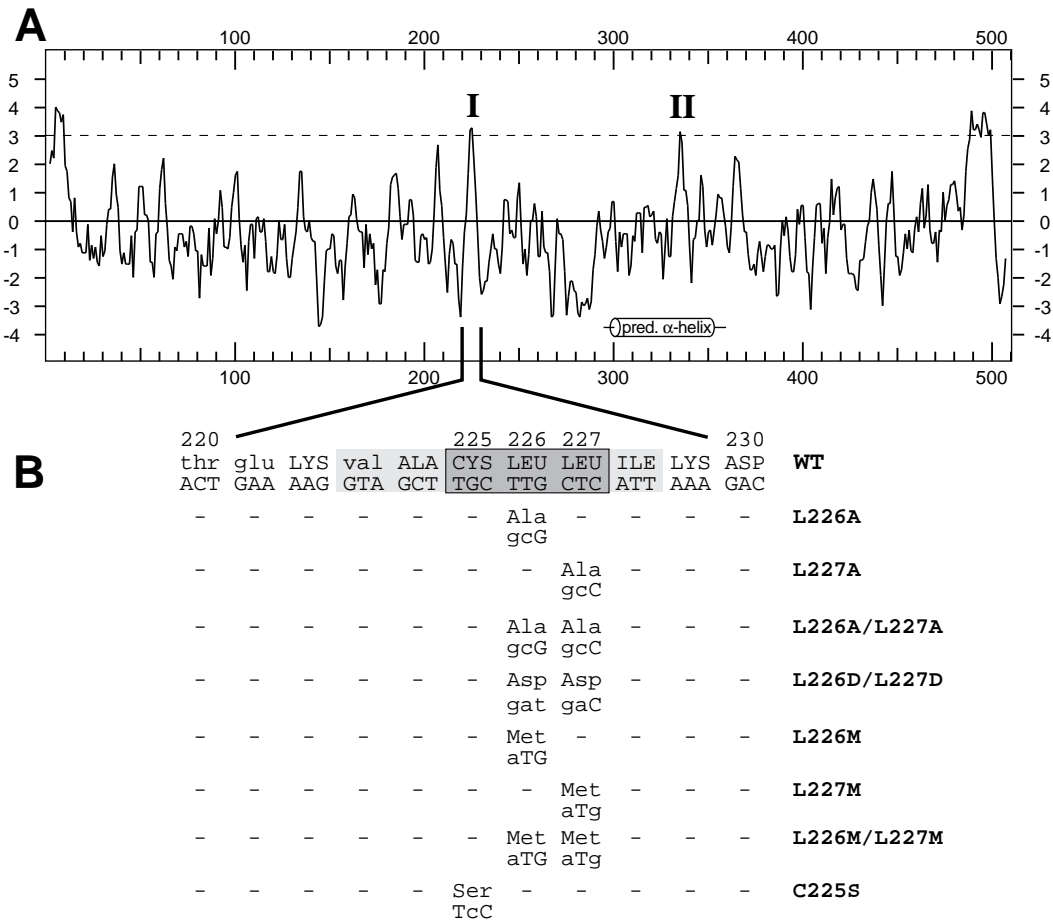
FIG. 3. Hydrophobicity profile of OpMNPV GP64 EFP and mutations in hydrophobic region I. (A) A Kyte-Doolittle hydrophobicity profile of OpMNPV GP64 EFP was generated using DNA Strider and a window size of five residues (20). Within the ectodomain of GP64 EFP, only two regions exceed an average hydrophobicity value of 3. Hydrophobic region I (peak I) is centered at amino acid 225. Hydrophobic region II (peak II) is centered at amino acid 335. A region containing a predicted amphipathic alpha-helix (amino acids 298 to 346; pred. α-helix) is also indicated on the hydrophobicity plot. The vertical scale indicates Kyte-Doolittle hydrophobicity values, and numbers on the horizontal scale represent GP64 EFP amino acid numbers. (B) Amino acid substitution mutations were generated in region I of the wt OpMNPV GP64 EFP. The wt amino acid and corresponding nucleotide sequence for OpMNPV GP64 EFP region I are shown in the top lines. The locations of amino acid substitution mutations are shown below. In the top line, uppercase amino acids indicate identity between the OpMNPV, CfMNPV, and AcMNPV GP64 EFPs. The light gray box indicates the 6 hydrophobic amino acids of region I, and the dark gray box shows the three core amino acid positions selected for mutagenesis. Uppercase nucleotides indicate the wt OpMNPV sequence, and lowercase nucleotides indicate the oligonucleotide-directed base changes. The names of GP64 EFP proteins containing the indicated amino acid substitution mutations are listed on the right.

225, serine was substituted for Cys-225 (C225S mutation). The C225S mutation disrupted GP64 EFP oligomerization, as trimer I and trimer II bands were not detected (Fig. 4A, lane 9). In addition, this mutation resulted in an approximately 55% reduction of surface-localized GP64 EFP compared with that of the wt protein (Fig. 4B, column 9). In the syncytium formation assay, GP64 EFP with the C225S mutation did not exhibit membrane fusion activity (Fig. 4C, C225S). Thus, because GP64 EFP with the C225S mutation failed to oligomerize correctly, it is likely that this Cys residue is required in the folding pathway or for disulfide bonding in the native oligomeric state. Due to the defect in oligomerization, we could not assess whether the hydrophobic nature of Cys-225 contributes to the fusion activity of GP64 EFP.

Alteration of pH required for fusion activity. To further investigate the effects of region I hydrophobicity, the pH required to trigger membrane fusion activity was examined in the region I GP64 EFP mutants that retained fusion activity. Transfected Sf9 cells expressing wt GP64 EFP or GP64 EFPs containing region I mutations were exposed to various pHs from 5.0 to 6.0 for 5 min; they were then incubated for 2 h in TNM-FH medium and scored for the presence of syncytia (Table 1). In this assay, the membrane fusion activity of wt GP64 EFP was triggered at pH 5.8 and below. In contrast, the fusion activity of GP64 EFPs containing region I substitutions was triggered only by more acidic pH values. In general, a somewhat graded effect was observed, with decreasing hydrophobicity at positions 226 and 227 requiring more acidic pH to trigger fusion activity (Table 1). Interestingly, GP64 EFP with the L227A substitution required a more acidic pH to trigger fusion activity than did GP64 EFP with the L226A substitution, suggesting that GP64 EFP fusion activity may be more sensitive to the level of hydrophobicity at position 227 than that at position 226.

Antibody inhibition of fusion activity. To confirm the role of hydrophobic region I by a complementary technique, we examined the ability of anti-region I antibodies to block or inhibit the membrane fusion activity of GP64 EFP. To accomplish this, a peptide containing region I and 14 adjacent residues of OpMNPV GP64 EFP (Fig. 5A, amino acids 222 to 241) was
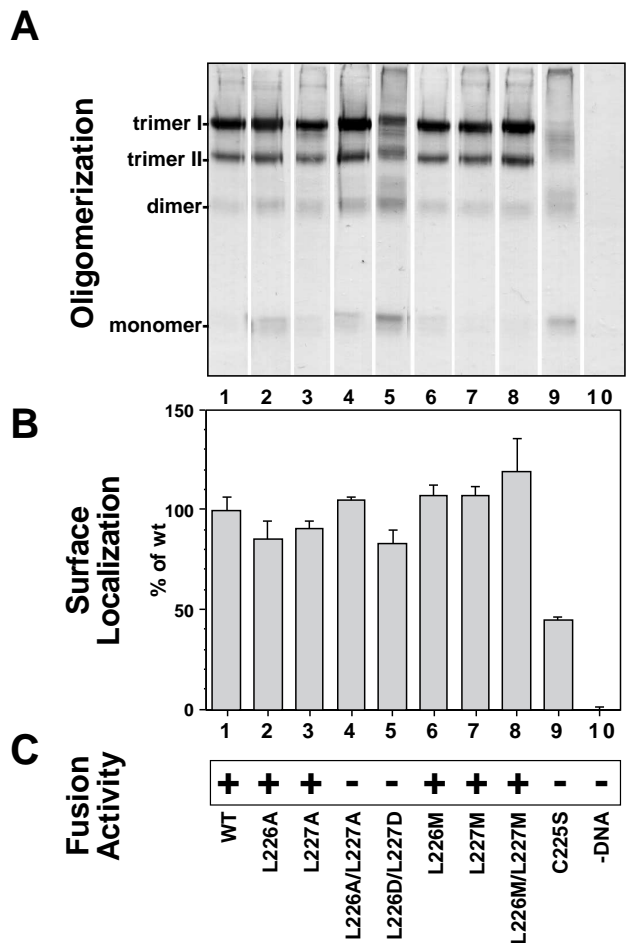
A

B

C

FIG. 4. Analysis of oligomerization, surface localization, and fusion activity of GP64 EFP containing substitution mutations in hydrophobic region I. (A) Western blots of GP64 EFP containing region I mutations. Sf9 cells were transfected with plasmids encoding GP64 EFP region I mutations and then lysed and electrophoresed under nonreducing conditions. Oligomeric forms of GP64 EFP were detected by Western blot analysis using MAb AcV5. The positions of GP64 EFP oligomers and GP64 EFP monomers are indicated on the left. Cells were transfected with either a wt OpMNPV GP64 EFP construct (lane 1) or with OpMNPV GP64 EFP constructs containing the region I mutations (lanes 2 to 9) indicated below panel C. Lane 10 shows a negative control of mock-transfected cells. Except for the blot in lane 3 (which was run on a separate gel), all samples shown are from the same blot. The positions of molecular size markers are indicated on the right. The markers used were (from top to bottom): Myosin, 200,000 Da; β-galactosidase, 116,250 Da; phosphorylase *b*, 97,400 Da; and bovine serum albumin, 66,200 Da. (B) Relative levels of GP64 EFP at the cell surface were detected by CELISA. Bars represent the mean CELISA signal (optical density at 405 nm) from three replicate wells normalized to the mean CELISA signal from wt GP64 EFP (100%). Error bars represent standard deviation. Order of samples is identical to that in panels A and C. (C) Fusion activity of wt and mutant GP64 EFPs was analyzed by a syncytium formation assay. Transfected cells expressing wt GP64 EFP or GP64 EFP containing region I mutations were exposed to pH 5.0 and examined for membrane fusion. A plus sign indicates the presence of multinuclear syncytia containing five nuclei or more. As a negative control, mock-transfected cells (-DNA) were also examined in the syncytium formation assay.

synthesized and used to produce a polyclonal rabbit antiserum. Antipeptide antibodies were affinity purified with the same peptide coupled to agarose beads. Affinity-purified antibodies reacted with the wt OpMNPV GP64 EFP and with mutant GP64 EFPs containing the region I substitutions on Western blots (data not shown). To determine if antibodies to this 20-amino-acid region could inhibit the fusion activity of GP64

TABLE 1. Membrane fusion activity at various pH[a]

Mutation	pH					
	5.0	5.2	5.4	5.6	5.8	6.0
wt	+	+	+	+	+	−
L226M	+	+	+	+	−	−
L227M	+	+	+	+	−	−
L226M/L227M	+	+	+	−	−	−
L226A	+	+	+	−	−	−
L227A	+	−	−	−	−	−

[a] pH requirement for fusion activity of wt GP64 EFP and GP64 EFPs containing mutations in region I. Sf9 cells were transfected with plasmids encoding the wt GP64 EFP or GP64 EFPs containing the indicated region I substitution mutations. Replicate wells were then tested in the syncytium formation assay, using a 5-min exposure to the indicated pH values. A plus sign indicates that syncytia containing five or more nuclei were detected.

EFP, transfected Sf9 cells expressing wt OpMNPV GP64 EFP were incubated with the anti-region I peptide antibodies for 1 h prior to analysis by syncytium formation assay. In transfected cells that had been incubated with the antipeptide antibodies, syncytium formation was completely inhibited (Fig. 5B). To confirm the specificity of the inhibition, a parallel assay was performed in which the affinity-purified antibodies were preadsorbed with an excess of free peptide prior to incubation with transfected cells. When control cells expressing wt GP64 EFP were incubated with the preadsorbed antibodies prior to the syncytium formation assay, normal membrane fusion and syncytium formation were observed (Fig. 5C). Additional negative controls included incubation of transfected cells with buffer alone or with free peptide alone. These negative controls also resulted in normal levels of syncytium formation (data not shown). These results demonstrate that antibodies to the 20-amino-acid region containing region I (amino acids 222 to 241 of OpMNPV GP64 EFP) are capable of reacting with GP64 EFP molecules on the surfaces of transfected cells and can inhibit the membrane fusion activity of wt OpMNPV GP64 EFP.

Antibody interference with viral infectivity. To determine if binding of the anti-region I peptide antibodies could neutralize or interfere with the infectivity of budded OpMNPV virions, we used a CELISA to detect GP64 EFP early gene expression as an indicator of viral entry into host cells (see Materials and Methods). In control experiments with *L. dispar* cells infected at an MOI of 20 and fixed at the end of a 1-h infection, GP64 EFP from the infecting virions was not detectable. Thus, at an MOI of ≤20, GP64 EFP detected at 20 h postinfection results from successful viral entry and early gene expression. To generate a standard curve of GP64 EFP expression and to demonstrate that detection of newly synthesized GP64 EFP was proportional to viral entry into host cells (gene dosage), cells were infected at increasing MOIs of from 0.01 to 10. These results (Fig. 6A) indicate that this assay detects newly synthesized GP64 EFP and that the level of GP64 EFP detected is proportional to the input gene dosage from an MOI of 0.1 to 10.

To detect neutralization or interference with infectivity caused by anti-region I peptide antibody binding, OpMNPV budded virions sufficient to yield an MOI of 5 were incubated with affinity-purified anti-region I antibodies for 1 h prior to infection of *L. dispar* cells. As negative controls, virions were incubated with antibodies preadsorbed with excess peptide, with peptide only, or with buffer only. As a measure of the effect of each treatment on viral entry, we calculated the effective MOI from the level of GP64 EFP expression. The level

A

222

241

NH – KVACLLIKDDKADPNSVTREY – COOH

B

C

FIG. 5. Inhibition of GP64 EFP membrane fusion activity by treatment with anti-region I antibodies. (A) The amino acid sequence of a synthetic region I peptide used to generate polyclonal antisera is shown. The peptide consists of Op*M*NPV GP64 EFP amino acids 222 to 241 plus a C-terminal tyrosine residue used for conjugation. The 6-amino-acid hydrophobic region I is shaded. (B) Membrane fusion was inhibited and syncytia were not observed when transfected Sf9 cells expressing the wt Op*M*NPV GP64 EFP were treated with affinity-purified anti-region I antibodies prior to acidification at pH 5.0 (see Materials and Methods). (C) Membrane fusion was not inhibited, and syncytia were observed when Sf9 cells expressing the wt Op*M*NPV GP64 EFP were treated as described in the legend to panel B, but with anti-region I antibodies preadsorbed with excess free peptide. Panels B and C are phase-contrast photomicrographs. Bars, 150 μm.

of GP64 EFP expression from each treatment (Fig. 6B, OD_{405}) was plotted against the standard curve of GP64 EFP expression versus MOI (Fig. 6A) generated in the same experiment, to yield the effective MOI (Fig. 6C). Treatment of virions with anti-region I antibodies resulted in an effective MOI of 0.8, a reduction of 83% from the buffer control (Fig. 6C, compare Buffer with α-Reg. I PAb). Incubation with twice the amount of anti-region I antibodies (Fig. 6C, 2× α-Reg. I PAb) resulted in only a slightly lower effective MOI of 0.6. Thus, treatment of infectious virions with the anti-region I antibodies resulted in an approximately 83 to 87% reduction in infectivity, from an effective MOI of 4.6 (buffer treated) to an effective MOI of 0.6 to 0.8. These results confirm the role of GP64 EFP hydrophobic region I during the infection process.

Mutations in hydrophobic region II. Hydrophobic region II is located from amino acid 330 to 338, near the C-terminal end of a strongly predicted amphipathic alpha-helix that extends from approximately amino acid 298 to 346 (Fig. 3A and 7A). The amino acid sequence of the predicted alpha-helix contains a long heptad repeat (or leucine zipper), exhibiting one methionine and five leucine residues at every seventh position from amino acid 299 to 334 (Fig. 7A, arrowheads). The amino acid sequence also contains an a-d repeat (Fig. 7A, dots = a position, arrowheads = d position), which is typically found in alpha-helices that can form multistranded coiled-coils (in a heptad repeat of a-b-c-d-e-f-g, positions a and d are predominantly bulky and hydrophobic or neutral [9]). In a helical net representation of the sequence, six hydrophobic residues of region II form a cluster on one face of the predicted alpha-helix (Fig. 7B, circled amino acids). To examine the potential roles of the three major structural characteristics of this region, we generated substitution mutations to analyze (i) the heptad leucine repeat, (ii) the predicted alpha-helical structure, and (iii) the hydrophobic cluster of region II.

We first examined the effect of reducing the length of the heptad repeat by substituting alanine for either or both of the final heptad leucines in the repeat at positions 327 and 334 (Fig. 7C, L327A, L334A, and L327A/L334A). The effects of these mutations on GP64 EFP oligomerization, transport, and function are shown in Fig. 8. The single alanine substitutions at positions 327 or 334 did not prevent GP64 EFP oligomerization (Fig. 8A, lanes 2 and 3) or transport to the cell surface (Fig. 8B, columns 2 and 3). In addition, membrane fusion activity appeared normal (Fig. 8C, L327A and L334A). In contrast to the single alanine substitutions, double alanine substitutions at positions 327 and 334 (L327A/L334A) interfered with GP64 EFP oligomerization and transport (Fig. 8A, lane 4, and 8B, column 4) and no fusion activity was detectable (Fig. 8C, L327A/L334A). Because oligomerization and transport were defective in GP64 EFP containing the double alanine substitutions, the effect on membrane fusion could not be addressed. However, these data clearly demonstrate that substitution of alanine for the two terminal leucines of the heptad repeat prevented oligomerization of GP64 EFP, suggesting that the heptad leucine repeat may be required for the oligomerization of GP64 EFP.

During the generation of mutant L334A, we recovered a spontaneous mutation that resulted in the additional substitution of serine for Met-331 (mutant M331S/L334A). The fortuitous serine substitution at position 331 created a new N-linked glycosylation signal at Asn-329, which is located on the hydrophilic face of the predicted alpha-helix. GP64 EFP containing the double substitution M331S/L334A was defective for oligomerization and transport (Fig. 8A, lane 8, and 8B, column 8). The monomer band on Western blots exhibited decreased electrophoretic mobility, with an estimated molecular size of approximately 68 kDa, suggesting that the new glycosylation signal was utilized for carbohydrate addition. In the fusion

A

EFP expression vs. log MOI

B

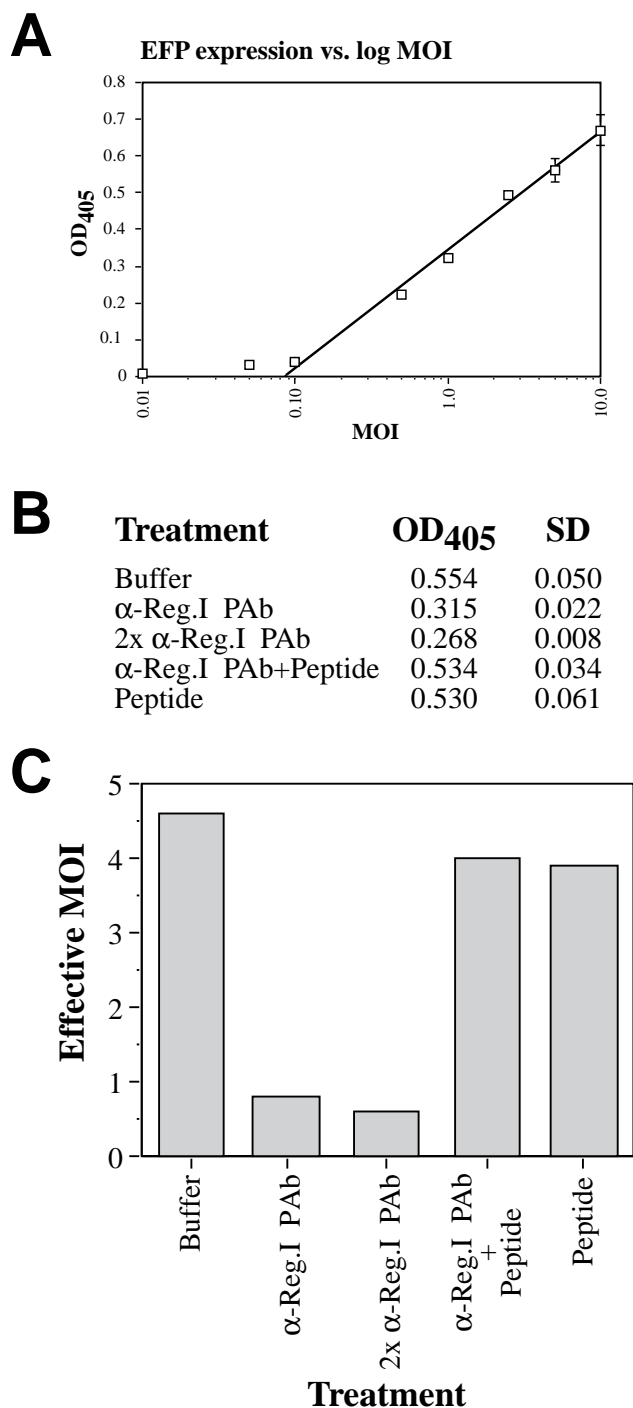| Treatment	OD$_{405}$	SD
Buffer	0.554	0.050
α-Reg.I PAb	0.315	0.022
2x α-Reg.I PAb	0.268	0.008
α-Reg.I PAb+Peptide	0.534	0.034
Peptide	0.530	0.061

C

FIG. 6. Inhibition of viral entry by treatment with anti-region I antibodies. (A) Detection of newly synthesized GP64 EFP was used as a measure of viral entry into host cells. *L. dispar* cells were infected with Op*M*NPV budded virions at increasing MOIs. Cells were fixed and permeabilized at 20 h postinfection, and relative levels of GP64 EFP expression were determined by CELISA with MAb AcV5. The graph shows a standard curve of MOI versus GP64 EFP detected and demonstrates the proportional relationship between MOIs of 0.1 to 10 and GP64 EFP detection. (Note: GP64 EFP from the virus inoculum is not detectable in this assay [data not shown]). (B) Effects of antibody treatments on GP64 EFP expression. Optical density at 405 nm (OD$_{405}$) values from CELISA detection of GP64 EFP after infection with virions (MOI, 5) that were treated with either buffer, anti-region I peptide antibodies (α-Reg. I PAb and 2× α-Reg. I PAb), anti-region I peptide antibodies preadsorbed with region I peptide (α-Reg. I PAb+Peptide), or region I peptide (Peptide). After treatment, virions were used to infect *L. dispar* cells and GP64 EFP levels were determined by CELISA at 20 h postinfection, as described above. Mean OD$_{405}$ values and standard deviations

assay, the M331S/L334A mutant was negative, as would be expected from the defects in oligomerization and transport (Fig. 8C, M331S/L334A). Thus, while the L334A mutation alone did not inhibit GP64 EFP oligomerization, the addition of a glycosylation site did prevent oligomerization.

We next examined the role of the predicted alpha-helical structure near hydrophobic region II. To disrupt the predicted alpha-helical conformation, a helix-destabilizing amino acid (proline) was substituted for either or both leucines at positions 327 and 334 (Fig. 7C; L327P, L334P, and L327P/L334P). The effects of these mutations are summarized in Fig. 8A (lanes 5 to 7). Both single and double proline substitutions interfered with GP64 EFP oligomerization (Fig. 8A, lanes 5 to 7) and with transport to the cell surface (Fig. 8B, columns 5 to 7), and no membrane fusion activity was detected from any of the proline substitutions (Fig. 8C, L327P, L334P, and L327P/L334P). As with the mutations discussed above, the lack of normal surface localization precludes an analysis of fusion activity. The results of helix-disrupting amino acid substitutions suggest that the predicted alpha-helical structure near hydrophobic region II may also be important for the correct folding and oligomerization of GP64 EFP.

Six residues of hydrophobic region II form a hydrophobic cluster on one face of the predicted alpha-helix (Fig. 7B, circled amino acids). To reduce the overall hydrophobicity of this cluster without disrupting the predicted alpha-helix, alanine was substituted for hydrophobic amino acids of the cluster at either two positions (Fig. 7C, L334A/I335A) or four positions (Fig. 7C, M330A/M331A/L334A/I335A). Both of these multiple substitution mutations in hydrophobic region II interfered with GP64 EFP oligomerization (Fig. 8A, lanes 9 and 10) and surface localization (Fig. 8B, columns 9 and 10). Fusion activity was not detectable in the syncytium formation assay (Fig. 8C, L334A/I335A and M330A/M331A/L334A/I335A). However, the lack of significant surface localization again precludes an analysis of fusion activity by these methods.

Thus, three types of mutations in hydrophobic region II resulted in defective oligomerization of GP64 EFP. These included mutations that (i) reduced the heptad repeat of leucine residues, (ii) disrupted the predicted alpha-helix, or (iii) reduced the hydrophobicity on one face of the predicted helix. Thus, these data indicate that the predicted amphipathic alpha-helical structure at amino acids 298 to 346 (and the heptad leucine repeat) forms an oligomerization domain which includes hydrophobic region II. This interpretation was supported by the analysis of two large deletions within the ectodomains of the Ac*M*NPV and Op*M*NPV GP64 EFPs (Fig. 9). An in-frame deletion of 77 amino acids from the Op*M*NPV GP64 EFP (amino acids 264 to 340, Fig. 9A), removing the predicted amphipathic alpha-helix and hydrophobic region II, prevented GP64 EFP oligomerization when expressed in transfected cells. However, a large in-frame deletion of 250 amino acids of Ac*M*NPV GP64 EFP (amino acids 29 to 278, Fig. 9B), removing most of the N-terminal half of Ac*M*NPV GP64 EFP, did not prevent the formation of disulfide-bonded dimers and trimers (data not shown). Thus, one GP64 EFP construct containing only 47% of the wt ectodomain (and retaining the predicted amphipathic helix and hydrophobic region II) was

(SD) from CELISA detection of GP64 EFP in three replicate wells are listed beside each treatment. (C) Effective MOI determinations. To measure the effect of each treatment on viral entry into host cells, the relative levels of GP64 EFP detected (panel B) were used to determine an effective MOI by interpolating from the standard curve shown in panel A. Virion treatments are described in the legend to panel B.
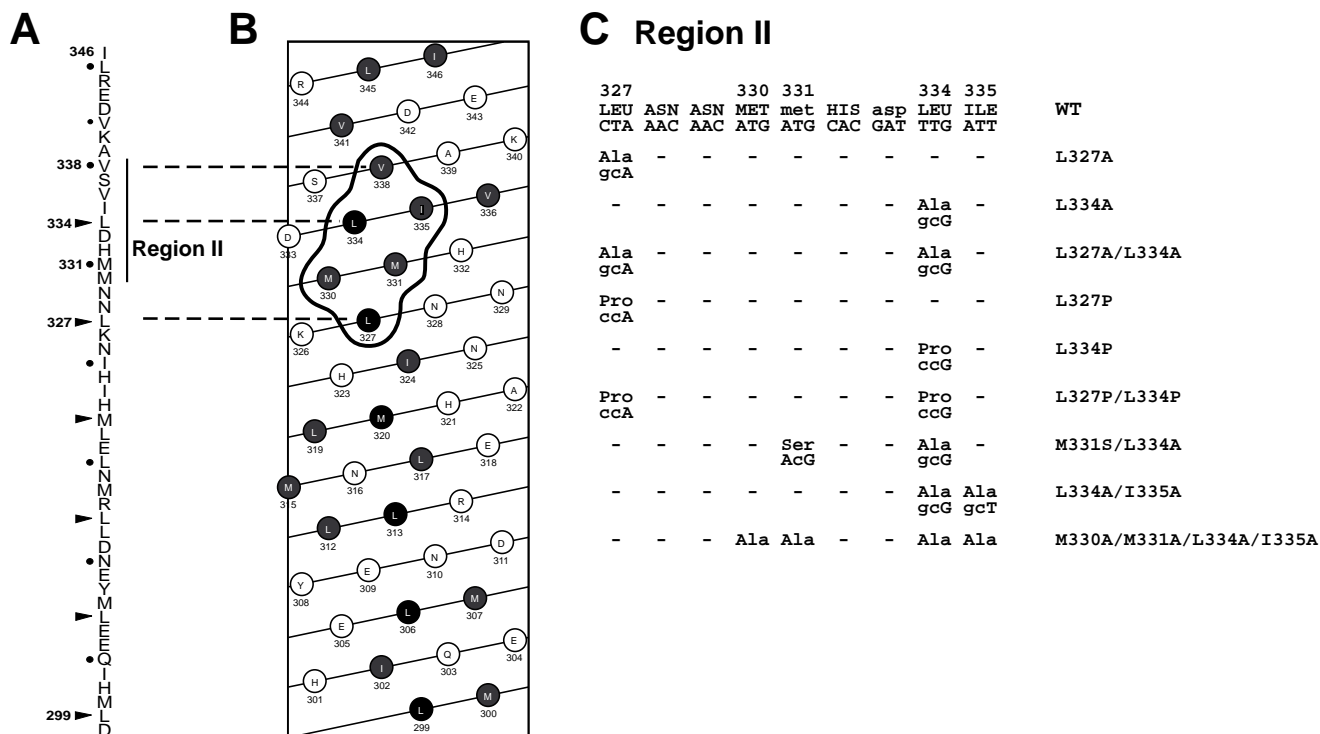
FIG. 7. Substitution mutations within hydrophobic region II and the predicted amphipathic alpha-helix. (A) Sequence of the predicted amphipathic alpha-helix of Op*M*NPV GP64 EFP (amino acids 299 to 346), with the highly hydrophobic region II (vertical line) indicated on the right. Heptad repeats of leucine/methionine residues (arrowheads), a-d repeat residues (filled circles), and amino acid numbers are on the left. (B) Helical net representation of the predicted amphipathic helix from amino acids 299 to 346. Hydrophobic amino acids (I, L, M, and V) are indicated by solid circles and other amino acids are indicated by open circles. The hydrophobic amino acids of region II (Fig. 3A) are shown as a cluster of residues on one face of the predicted alpha-helix (circled amino acids). (C) Amino acid substitution mutations were generated in region II of the wt Op*M*NPV GP64 EFP. The wt Op*M*NPV region II amino acid and corresponding nucleotide sequences are shown in the top two lines. The locations of amino acid substitution mutations are shown below. In the top line, uppercase amino acids indicate identity between the Op*M*NPV, Cf*M*NPV, and Ac*M*NPV GP64 EFPs. Met-331 is replaced by Leu in the Ac*M*NPV and Cf*M*NPV GP64 EFPs. In the lines below, lowercase nucleotides indicate the oligonucleotide-directed base changes. The names of GP64 EFPs containing the indicated amino acid substitution mutations are listed on the right.

capable of oligomerization. In contrast, another GP64 EFP construct with a more discrete deletion of the predicted amphipathic helix and region II was defective for oligomerization. Thus, these deletion data, in combination with several substitution mutation strategies, support the conclusion that the amphipathic alpha-helix is required for the oligomerization of GP64 EFP.

DISCUSSION

To identify and analyze functional domains in the baculovirus GP64 EFP, we used mutagenesis strategies involving insertions, deletions, and single or multiple amino acid substitutions. Of 11 insertion mutations examined (7 linker insertions and 4 linker reductions), 9 prevented oligomerization and surface localization of GP64 EFP. These results indicate that the process of GP64 EFP folding and oligomerization is sensitive to even small insertions in the amino acid sequence.

The results of amino acid substitutions in hydrophobic region II and the predicted amphipathic helix suggest that this region is required for oligomerization and thus constitutes an oligomerization domain. Oligomerization of GP64 EFP was prevented by several types of substitutions in this region. These included (i) helix-disrupting substitutions, (ii) reduction of the length of the heptad repeat, and (iii) reduction in the hydrophobicity of region II. In addition, a discrete deletion of the predicted alpha-helical region and hydrophobic region II prevented the oligomerization of Op*M*NPV GP64 EFP, whereas

deletion of most of the N-terminal half of Ac*M*NPV GP64 EFP did not prevent oligomerization. Together, the results of these experiments suggest that the three major features of this region, the heptad leucine repeat, the predicted alpha-helical structure, and the hydrophobic cluster on one face of the predicted helix, all play a role in the proper folding and oligomerization of GP64 EFP.

Mutations in baculovirus GP64 EFP hydrophobic region II which interfered with oligomerization also interfered with transport to the cell surface, similar to other viral fusion proteins that require oligomerization for cellular transport (10). However, because of the lack of GP64 EFP surface localization, the fusion activity of GP64 EFPs containing mutations in hydrophobic region II could not be tested. Thus, the results of this study do not rule out a direct role for region II in membrane fusion. In several other viral membrane fusion proteins, amphipathic alpha-helices appear to play direct roles in membrane fusion. Recent experiments (36) and resulting models (6) of membrane fusion mediated by the influenza virus hemagglutinin (HA) protein suggest that in addition to the N-terminal fusion peptide, an amphipathic helix in HA may directly interact with host target membranes during fusion (6). Site-directed mutagenesis studies of human immunodeficiency virus gp41 and measles virus F protein indicate that the leucine zippers (amphipathic helices) found in these fusion proteins are required for membrane fusion activity (5, 11). Future studies with baculovirus GP64 EFP will address the potential role
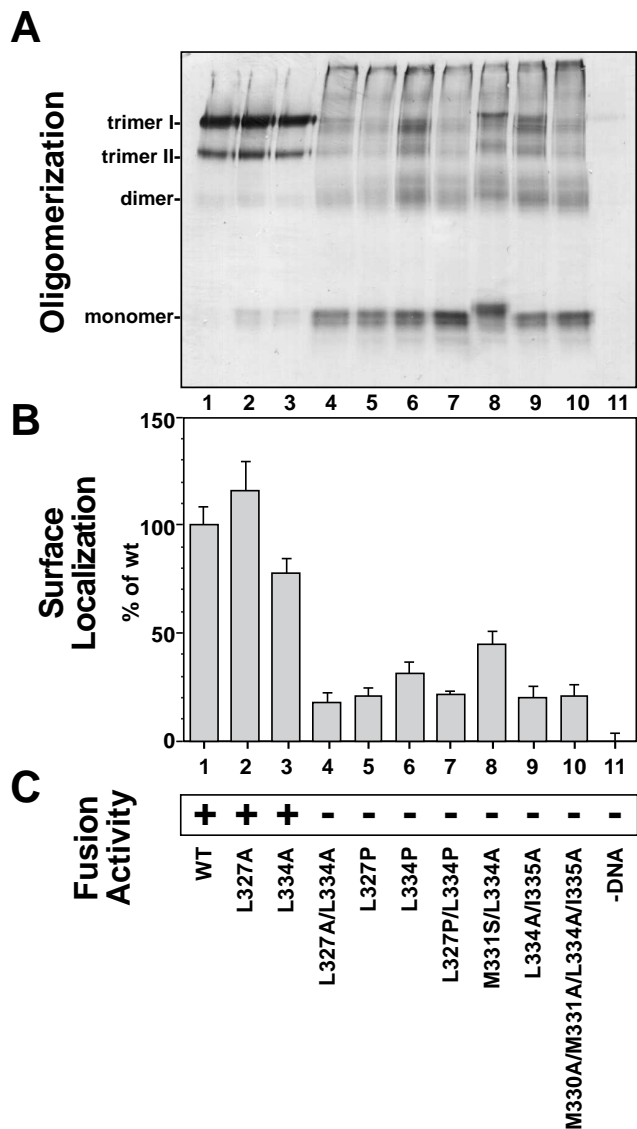
FIG. 8. Analysis of oligomerization, surface localization, and fusion activity of GP64 EFP containing mutations in hydrophobic region II. (A) Western blots of GP64 EFP containing region II mutations. Sf9 cells were transfected with plasmids encoding GP64 EFP region II mutations and then lysed and electrophoresed under nonreducing conditions. Oligomeric forms of GP64 EFP were detected by Western blot analysis with MAb AcV5. The positions of GP64 EFP oligomers and GP64 EFP monomers are indicated on the left. Cells were transfected with either a wt Op*M*NPV GP64 EFP construct (lane 1) or with Op*M*NPV GP64 EFP constructs containing the region II mutations (lanes 2 to 10) indicated below panel C. Lane 11 shows a negative control of mock-transfected cells. The positions of molecular size markers are indicated on the right, as described in the legend to Fig. 4A. (B) Relative levels of GP64 EFP at the cell surface were detected by CELISA. Bars represent the mean CELISA signal (optical density at 405 nm) from three replicate wells normalized to the mean CELISA signal from wt GP64 EFP (100%). Error bars represent standard deviation. The order of samples is identical to that in panels A and C. (C) Fusion activity of wt and mutant GP64 EFPs was analyzed by a syncytium formation assay, as described in the legend to Fig. 4C. A plus sign indicates the presence of multinuclear syncytia containing five nuclei or more. As a negative control, mock-transfected cells (-DNA) were also examined in the syncytium formation assay.

of hydrophobic region II (and the predicted amphipathic helix) in fusion activity.

In the baculovirus GP64 EFP, hydrophobic region I exhibits the highest average hydrophobicity in the ectodomain. Hydrophobic region I is composed of a linear sequence of 6 hydro-

phobic amino acids. Amino acid substitutions that neutralized or altered the hydrophobicity of region I did not prevent oligomerization or surface localization of GP64 EFP but abolished acid-induced membrane fusion activity. This result functionally defines hydrophobic region I as a fusion domain of the baculovirus GP64 EFP. This conclusion is supported by experiments using affinity-purified polyclonal antibodies directed against a synthetic peptide containing region I. The affinity-purified antibodies completely inhibited the membrane fusion activity of wt GP64 EFP expressed in transfected insect cells. This result demonstrates that the 20-amino-acid region containing hydrophobic region I is accessible to antibodies and therefore may be exposed on the surface of GP64 EFP. More importantly, antibody binding to this region is sufficient to inhibit the membrane fusion activity of GP64 EFP. The role of hydrophobic region I during the infection process is supported by experiments that showed decreased viral entry into host cells when virions were treated with the affinity-purified anti-region I antibodies. Previous studies have shown that the neutralizing MAb AcV1 does not prevent the binding of baculovirus virions to host cells but appears to neutralize infection at a later stage (32). In fusion inhibition experiments with transfected cells expressing wt Ac*M*NPV GP64 EFP, we found that, like the anti-region I polyclonal antibodies, MAb AcV1 inhibited the membrane fusion activity of GP64 EFP (unpublished results). However, because AcV1 recognizes a conformational epitope, the epitope could not be mapped by the methods used in this study and thus it is not clear whether AcV1 binds to a functionally important site of GP64 EFP or simply constrains a conformational change.

The baculovirus GP64 EFP fusion domain identified in this study is an internal amino acid sequence and is similar in several respects to the internal fusion domains of Semliki Forest virus (SFV) E1 glycoprotein and vesicular stomatitis virus (VSV) G protein (19, 37). The amino acid sequences of the SFV and VSV fusion domains are highly conserved within the alphaviruses and vesiculoviruses, respectively, as is hydrophobic region I within the three known baculovirus GP64 EFPs. Site-directed mutagenesis of particular conserved residues in the SFV or VSV fusion domains abolished fusion activity without affecting transport to the cell surface, whereas substitutions of other conserved residues altered the pH optima for fusion activity to more acidic values (19, 37). In addition, the fusion domains of both VSV and SFV are flanked by charged amino acids, as is the baculovirus GP64 EFP fusion domain. One notable difference between the fusion domains of VSV and SFV and that of the GP64 EFP is size. The SFV fusion domain consists of 21 uncharged or nonpolar amino acids and the VSV fusion domain is 14 amino acids long, whereas the GP64 EFP fusion domain consists of 6 hydrophobic amino acids. However, as the detailed roles of these fusion domains in membrane fusion are not yet known, the functional significance of fusion domain size is not clear.

The close link between the hydrophobicity of baculovirus GP64 EFP region I and the membrane fusion activity is highlighted by the effects of substitutions which altered the hydrophobicity of region I but did not abolish fusion activity. GP64 EFP containing substitutions that reduced hydrophobicity in region I required a more acidic pH value to trigger the membrane fusion activity. Several possible mechanisms may explain the differences in pH requirements for observed membrane fusion in the syncytium formation assay. (i) Hydrophobic region I may directly interact with membrane lipids during initial stages of the fusion reaction, similar to the proposed interaction of the influenza virus HA fusion peptide with the adjacent membrane. In this case, reducing the hydrophobicity of region
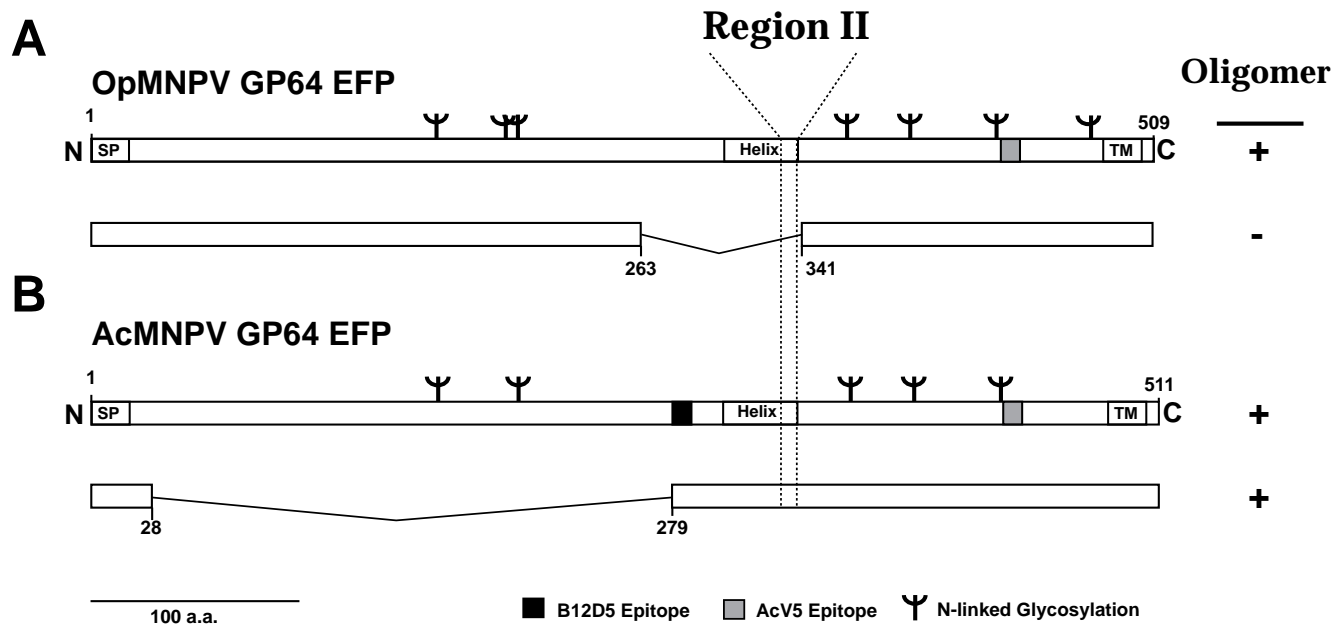
FIG. 9. Effects of large deletions in the OpMNPV and AcMNPV GP64 EFPs on oligomerization. Horizontal bars represent wt OpMNPV and AcMNPV GP64 EFPs. Proteins encoded by in-frame deletion subclones are illustrated below the wt GP64 EFP genes. Boxes represent coding regions and thin single lines (V-shaped) indicate the locations of deleted portions of the protein. On the right, + indicates the detection of oligomerized forms of GP64 EFP by electrophoresis on nonreducing SDS-polyacrylamide gels and Western blot analysis as described in Materials and Methods. (A) Schematic of the major features of the OpMNPV GP64 EFP. The location of hydrophobic region II is indicated above the diagram (dashed lines). The protein encoded by a deletion subclone is shown below. The deletion subclone does not contain amino acids 264 to 340 or region II, and no oligomerization was observed. (B) The major features of the AcMNPV GP64 EFP are shown in the top schematic, and a large deletion subclone is indicated below. The protein encoded by the deletion subclone does not contain amino acids 29 to 278 but does contain the predicted amphipathic helix and hydrophobic region II. Oligomeric forms of the AcMNPV GP64 EFP deletion protein were detected.

I may interfere with or reduce the efficiency of the initial interaction of GP64 EFP with an adjacent membrane. (ii) Hydrophobic region I may be required later in the membrane fusion process, during the membrane apposition phase (in which membranes are brought in close apposition [6]) or during formation of the initial pore (38). (iii) Alternatively, the hydrophobicity of region I may act to destabilize the native conformation of GP64 EFP such that a conformational change of wt GP64 EFP to the fusogenic state occurs near pH 5.8. Because mutant forms of GP64 EFP that are less hydrophobic in region I may be more stable, the conformational change of mutant GP64 EFP to the fusogenic state may require more acidic pH values. Elucidation of the GP64 EFP membrane fusion mechanism and the role of hydrophobic region I will require a more detailed dissection of the fusion event. Because baculovirus-infected cells have been used as a model system for the study of pore formation kinetics during membrane fusion (8, 18, 29), it should now be possible to examine more specifically the role of hydrophobicity in region I during the merger of adjacent membranes and formation of the fusion pore.

REFERENCES

1. **Anderson, S.** 1981. Shotgun DNA sequencing using cloned DNase I-generated fragments. Nucleic Acids Res. **9:**3015–3027.
2. **Blissard, G. W., and G. F. Rohrmann.** 1989. Location, sequence, transcrip-
   tional mapping, and temporal expression of the *gp64* envelope glycoprotein gene of the *Orgyia pseudotsugata* multicapsid nuclear polyhedrosis virus. Virology **170:**537–555.
3. **Blissard, G. W., and G. F. Rohrmann.** 1991. Baculovirus *gp64* gene expression: analysis of sequences modulating early transcription and transactivation by IE1. J. Virol. **65:**5820–5827.
4. **Blissard, G. W., and J. R. Wenz.** 1992. Baculovirus GP64 envelope glycoprotein is sufficient to mediate pH-dependent membrane fusion. J. Virol. **66:**6829–6835.
5. **Buckland, R., E. Malvoisin, P. Beauverger, and F. Wild.** 1992. A leucine zipper structure present in the measles virus fusion protein is not required for its tetramerization but is essential for fusion. J. Gen. Virol. **73:**1703–1707.
6. **Carr, C. M., and P. S. Kim.** 1994. Flu virus invasion: halfway there. Science **266:**234–236.
7. **Chambers, P., C. R. Pringle, and A. J. Easton.** 1990. Heptad repeat sequences are located adjacent to hydrophobic regions in several types of virus fusion glycoproteins. J. Gen. Virol. **71:**3075–3080.
8. **Chernomordik, L. V., S. S. Vogel, A. Sokoloff, H. O. Onaran, E. A. Leikina, and J. Zimmerberg.** 1993. Lysolipids reversibly inhibit Ca+2-, GTP- and pH-dependent fusion of biological membranes. FEBS Lett. **318:**71–76.
9. **Cohen, C., and D. A. D. Parry.** 1986. Alpha-helical coiled coils: a widespread motif in proteins. Trends Biochem. Sci. **11:**245–248.
10. **Doms, R. W., R. A. Lamb, J. K. Rose, and A. Helenius.** 1993. Folding and assembly of viral membrane proteins. Virology **193:**545–562.
11. **Dubay, J. W., S. J. Roberts, B. Brody, and E. Hunter.** 1992. Mutations in the leucine zipper of the human immunodeficiency virus type 1 transmembrane glycoprotein affect fusion and infectivity. J. Virol. **66:**4748–4756.
12. **Harlow, E., and D. Lane.** 1988. Antibodies: a laboratory manual. Cold Spring Harbor Laboratory, Cold Spring Harbor, N.Y.
13. **Hill, J. E., and P. Faulkner.** 1994. Identification of the gp67 gene of a baculovirus pathogenic to the spruce budworm, *Choristoneura fumiferana* multinucleocapsid nuclear polyhedrosis virus. J. Gen. Virol. **75:**1811–1813.
14. **Hohmann, A. W., and P. Faulkner.** 1983. Monoclonal antibodies to baculovirus structural proteins: determination of specificities by Western blot analysis. Virology **125:**432–444.
15. **Keddie, B. A., G. W. Aponte, and L. E. Volkman.** 1989. The pathway of infection of *Autographa californica* nuclear polyhedrosis virus in an insect host. Science **243:**1728–1730.
16. **Keddie, B. A., and L. E. Volkman.** 1985. Infectivity difference between the two phenotypes of *Autographa californica* nuclear polyhedrosis virus: importance of the 64K envelope glycoprotein. J. Gen. Virol. **66:**1195–1200.

17. **Laemmli, U. K.** 1970. Cleavage of structural proteins during the assembly of the head of bacteriophage T4. Nature (London) **227:**680–685.
18. **Leikina, E., H. O. Onaran, and J. Zimmerberg.** 1992. Acidic pH induces fusion of cells infected with baculovirus to form syncytia. FEBS Lett. **304:** 221–224.
19. **Levy-Mintz, P., and M. Kielian.** 1991. Mutagenesis of the putative fusion domain of the Semliki Forest virus spike protein. J. Virol. **65:**4292–4300.
20. **Marck, C.** 1988. DNA Strider: a "C" program for the fast analysis of DNA and protein sequences on the Apple Macintosh. Nucleic Acids Res. **16:**1829–1836.
20a.**Oomens, A. G. P., S. A. Monsma, and G. W. Blissard.** Unpublished data.
21. **O'Reilly, D. R., L. K. Miller, and V. A. Luckow.** 1992. Baculovirus expression vectors, a laboratory manual. W. H. Freeman & Co., New York.
22. **Ray, F. A., and J. A. Nickoloff.** 1992. Site-specific mutagenesis of almost any plasmid using a PCR-based version of unique site elimination. BioTechniques **13:**342–346.
23. **Roberts, S. R., and J. S. Manning.** 1993. The major envelope glycoprotein of the extracellular virion of *Autographa californica* nuclear polyhedrosis virus possesses at least three distinct neutralizing epitopes. Virus Res. **28:**285–297.
24. **Roberts, T. E., and P. Faulkner.** 1989. Fatty acid acylation of the 67K envelope glycoprotein of a baculovirus *Autographa californica* nuclear polyhedrosis virus. Virology **172:**377–381.
25. **Smith, G. E., and M. D. Summers.** 1978. Analysis of baculovirus genomes with restriction endonucleases. Virology **89:**517–527.
26. **Summers, M. D., and G. E. Smith.** 1987. A manual of methods for baculovirus vectors and insect cell culture procedures. Texas Agricultural Experiment Station Bulletin no. 1555. College Station, Tex.
27. **Summers, M. D., and L. E. Volkman.** 1976. Comparison of biophysical and morphological properties of occluded and extracellular nonoccluded baculovirus from in vivo and in vitro host systems. J. Virol. **17:**962–972.
28. **Victoria, E. J., L. C. Mahan, and S. P. Masouredis.** 1977. Immunoglobulin G

disassembly during thermal denaturation in sodium dodecyl sulfate solutions. Biochemistry **16:**2566–2570.
29. **Vogel, S. S., E. A. Leikina, and L. V. Chernomordik.** 1993. Lysophosphatidylcholine reversibly arrests exocytosis and viral fusion at a stage between triggering and membrane merger. J. Biol. Chem. **268:**25764–25768.
30. **Volkman, L. E.** 1986. The 64K envelope protein of budded *Autographa californica* nuclear polyhedrosis virus. Curr. Top. Microbiol. Immunol. **131:** 103–118.
31. **Volkman, L. E., and P. A. Goldsmith.** 1984. Budded *Autographa californica* NPV 64K protein: further biochemical analysis and effects of postimmunoprecipitation sample preparation conditions. Virology **139:**295–302.
32. **Volkman, L. E., and P. A. Goldsmith.** 1985. Mechanism of neutralization of budded *Autographa californica* nuclear polyhedrosis virus by a monoclonal antibody: inhibition of entry by adsorptive endocytosis. Virology **143:**185–195.
33. **Volkman, L. E., P. A. Goldsmith, R. T. Hess, and P. Faulkner.** 1984. Neutralization of budded *Autographa californica* NPV by a monoclonal antibody: identification of the target antigen. Virology **133:**354–362.
34. **White, J. M.** 1990. Viral and cellular membrane fusion proteins. Annu. Rev. Physiol. **52:**675–698.
35. **Whitford, M., S. Stewart, J. Kuzio, and P. Faulkner.** 1989. Identification and sequence analysis of a gene encoding *gp67*, an abundant envelope glycoprotein of the baculovirus *Autographa californica* nuclear polyhedrosis virus. J. Virol. **63:**1393–1399.
36. **Yu, Y. G., D. S. King, and Y.-K. Shin.** 1994. Insertion of a coiled-coil peptide from influenza virus hemagglutinin into membranes. Science **266:**274–276.
37. **Zhang, L., and H. P. Ghosh.** 1994. Characterization of the putative fusogenic domain in vesicular stomatitis virus glycoprotein G. J. Virol. **68:**2186–2193.
38. **Zimmerberg, J., S. S. Vogel, and L. V. Chernomordik.** 1993. Mechanisms of membrane fusion. Annu. Rev. Biophys. Struct. **22:**433–466.